Liquid Crystals
Publication details, including instructions for authors and subscription information:
http://www.informaworld.com/smpp/title~content=t713926090

Synthesis and liquid crystalline structures of poly(L-lysine) containing undecanamidobiphenyl units in the side chains

Céline Guillermain; Bernard Gallot

Online publication date: 11 November 2010

To cite this Article Guillermain, Céline and Gallot, Bernard(2002) 'Synthesis and liquid crystalline structures of poly(L-lysine) containing undecanamidobiphenyl units in the side chains', Liquid Crystals, 29: 1, 141 — 153
To link to this Article: DOI: 10.1080/02678290110099439
URL: http://dx.doi.org/10.1080/02678290110099439

LIQUID CRYSTALS, 2002, VOL. 29, NO. 1, 141–153

Synthesis and liquid crystalline structures of poly(L-lysine) containing undecanamidobiphenyl units in the side chains

CÉLINE GUILLERMAIN and BERNARD GALLOT*
LMOPS-CNRS, BP.24, 69390 Vernaison, France

(*Received 6 July 2001; accepted 26 August 2001*)

In order to obtain liquid crystalline comb-like poly(L-lysine) bearing biphenylyl mesogenic groups in their side chains, we synthesized the 11-(biphenyl-4-carboxamido)undecanamido-L-lysine (KC10φφ) from L-lysine by a five step procedure and transformed the KC10φφ into its polymerizable cyclic derivative (the *N*-carboxyanhydride or NCA derivative) by the action of diphosgene. We homopolymerized the NCA of KC10φφ to obtain the polymer pKC10φφ and copolymerized it with the NCA of trifluoroacetyl-L-lysine (Kt) to obtain block copolymers pKt-pKC10φφ of various compositions. X-ray diffraction studies demonstrated the existence of mesophases for our homopolymers and copolymers, resolved the structure of the mesophases and established the influence of temperature and the composition of the copolymers on the structure of the mesophases. Homopolymers pKC10φφ exhibit, as a function of temperature, three phases (CrE_d, SmB_d and SmA_d) deriving from the β-pleated sheet structure of polypeptides and proteins. The presence of a pKt block in copolymers pKt-pKC10φφ transforms the smectic CrE_d structure into a SmA_d structure and, when the content of pKt block increases, into a bidimensional hexagonal structure similar to that of the homopolymers pKt.

1. Introduction

Recently we showed that poly(L-lysine) and poly(L-ornithine) bearing azobenzene units in their side chains exhibit thermotropic liquid crystalline properties [1–3]. The structure of their mesophases is of the smectic A type deriving from the β-pleated sheet structure of the polypeptides. For poly(L-lysine), the organization of the molecules in the smectic planes depends upon their degree of substitution [2]. For polymers where all the lysine units are substituted with azobenzene, the polypeptide main chains are arranged in their planes in the antiparallel β-structure and the side chains are perpendicular to the smectic layers. For polymers containing free lysine side chains, the smectic layer results from the superposition of two layers: one contains the hydrophilic free lysine side chains, the other one the azobenzene-modified lysine side chains and the polypeptidic main chains. In contrast, for partly substituted ornithines, there is no phase separation between azobenzene-modified side chains and free ornithine side chains in the smectic A structure [3].

In order to show that liquid crystalline structures can be obtained for polypeptides with other mesogenic groups than azobenzene, we decided to synthesize poly(L-lysine) bearing biphenylyl groups at the end of their side chains. To be sure that polymers bear a biphenylyl group at the end of every repeating unit, instead of performing a chemical modification of poly(L-lysine) we preferred to link through an amide bond an undecanamido-biphenyl group at the end of the lysine side chain, prepare the corresponding *N*-carboxyanhydride (NCA) and polymerize it.

In this paper we will describe the synthesis of the modified lysine: 11-(biphenyl-4-carboxamido)undecanamido-L-lysine (KC10φφ), the homopolymerization of the KC10φφ NCA and its copolymerization with the NCA of trifluoroacetyl-L-lysine (Kt) to obtain the homopolymers pKC10φφ and block copolymers pKt-pKC10φφ. We will also describe the liquid crystalline structures exhibited by the polymers and the influence of polymer composition and temperature on these structures.

2. Experimental

2.1. *Materials*

L-Lysine monohydrochloride and trichloromethyl chloroformate (diphosgene) were obtained from Fluka. Biphenyl-4-carboxylic acid, dicyclohexylcarbodiimide (DCC), *N*-hydroxysuccinimide (HOSu), 11-aminoundecanoic acid, copper carbonate and *S*-ethyl trifluorothioacetate were from Aldrich. Solvents were purified by classical methods.

*Author for correspondence; e-mail: lmops69@imaginet.fr

Liquid Crystals ISSN 0267-8292 print/ISSN 1366-5855 online © 2002 Taylor & Francis Ltd
http://www.tandf.co.uk/journals
DOI: 10.1080/02678290110099439

2.2. *Modified L-lysines*

2.2.1. *N^{ε}-Trifluoroacetyl-L-lysine*

To a 1 litre three-necked flask equipped with a magnetic stirrer and containing 450 ml of 1M NaOH were added first 74.15 g. of L-lysine monohydrochloride (0.406 mol), then 100 g of *S*-ethyl trifluorothioacetate (0.632 mol or 1.5 eq). The system was kept under argon and stirred for 6 h at room temperature. The white suspension of trifluoroacetyl-L-lysine (Kt) was filtered under vacuum and the filter cake washed several times with ethanol. After drying under vacuum at 40°C, 32.97 g of trifluoroacetyl-L-lysine (Kt) were obtained (yield 33.5%).

^{1}H NMR (250 MHz) (DMSO d_6, 350 K): 1.4–1.8 (m, 6H, $H_{3,4,5}$); 3.18 (t, 2H, H_6); 3.23 (s, 1H, H_2); 6.7 (s, 3H, $H_{a,b}$); 9.1 (sl, 1H, H_1). ^{13}C NMR (62.8 MHz) (DMSO d_6, 360 K): 22.21 (1C, C_4); 27.57 (1C, C_5); 30.63 (1C, C_3); 38.82 (1C, C_6); 53.82 (1C, C_2); 115.73 (q, $^1J_{CF} = 288.53$ Hz, C_8); 155.95 (q, $^2J_{CF} = 35.15$ Hz, C_7); 171.0 (1C, C_1).

2.2.2. *L-Lysine copper complex*

In a 1 litre three-necked flask equipped with a magnetic stirrer, 31.12 g of L-lysine monohydrochloride (0.165 mol) were dissolved in 220 ml of water. The solution was heated to boiling and 12.10 g of basic copper carbonate were added in small amounts to the lysine solution under reflux; the typical blue colour of the copper complex appeared. Heating was maintained for one hour, after which the system was cooled to room temperature and filtered to remove the excess of green copper carbonate; the filtrate of lysine complex was kept at room temperature without drying down.

2.2.3. *11-(Biphenyl-4-carboxamido)undecanamido-L-lysine*

*2.2.3.1. Biphenyl-4-carboxylic acid succinimidyl ester (**II**).* In a 2 litre three-necked flask equipped with a magnetic stirrer and containing a solution of 40 g of biphenyl-4-carboxylic acid (0.202 mol) in 1 litre of THF were added first 28.00 g of *N*-hydroxysuccinimide (0.244 mol) and then in small amounts 41.12 g of *N*,*N*′-dicyclohexylcarbodiimide (0.199 mol). The system was stirred for 5 h, the suspension was then filtered and white precipitate of *N*,*N*′-dicyclohexylurea (DCU) was washed with acetone. The filtrate was concentrated and further precipitated DCU was filtered off and washed. The process was repeated until the filtrate failed to show the characteristic band of DCU at 3328 cm^{-1} in the IR. The filtrate was further concentrated and poured into water at pH = 7. After filtration of the precipitate and drying at 45°C under vacuum, 32.12 g of the succinimidyl ester were obtained (yield 87.5%).

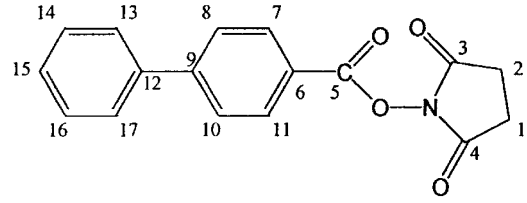

FTIR ester bands: 1769, 1731, 1201, 1073 cm^{-1}. ^{1}H NMR (250 MHz) (acetone d_6, $T = 25$°C): 2.98 (4H, $H_{1,2}$); 7.53–8.19 (9H, H_{arom}). ^{13}C (62.8 MHz) (acetone d_6): 27.13 (2C, $C_{1,2}$); 125.64 (1C, C_6); 128.87 (2C, $C_{8,10}$); 129.22 (3C, $C_{13,15,17}$); 130.77 (2C, $C_{14,16}$); 132.34 (2C, $C_{7,11}$); 140.74 (1C, C_{12}); 149.03 (1C, C_9); 163.41 (1C, C_5); 171.3 (2C, $C_{3,4}$).

*2.2.3.2. 11-(Biphenyl-4-carboxamido)undecanoic acid (**III**).* In a 3 litre three-necked flask equipped with a magnetic stirrer, 17.78 g of 11-aminoundecanoic acid (0.088 mol) were suspended in 883 ml of water, and 75 ml of acetone and 62.5 ml of triethylamine were added. Then 26.06 g of the succinimidyl ester **II** (0.088 mol) dissolved in 1165 ml of acetone were added in small amounts and finally 87.5 ml of TEA. The system was stirried at room temperature for 2 days. The acetone and TEA were then evaporated, water was added and the white suspension acidified to pH = 4 by addition of HCl. The 11-(biphenyl-4-carboxamido)undecanoic acid was filtered off, washed with water and dried; 24.73 g of white product were obtained (yield 74%).

^{1}H NMR (250 MHz) (DMSO d_6): 1.25–1.5 (m, 16H, $H_{3,4,5,6,7,8,9,10}$); 2.18 (t, 2H, H_2); 3.27 (q, 2H, H_{11}); 7.49–7.92 (9H, H_{arom}); 8.50 (t, 1H, H_1). ^{13}C NMR (62.8 MHz) (DMSO d_6): 24.67 (1C, C_3); 26.68 (1C, C_9); 28.74 (1C, C_4); 28.93* (1C, C_5); 28.96* (1C, C_8); 29.06** (1C, C_7); 29.15** (1C, C_7); 29.29 (1C, C_{10}); 33.86 (1C, C_2); 39.38 (1C, C_{11}); 126.52 (2C, $C_{20,24}$); 126.98 (2C, $C_{15,17}$); 127.98 (2C, $C_{14,18}$); 129.16 (2C, $C_{21,23}$); 133.678 (1C, C_{13}); 139.38 (1C, C_{19}); 142.66 (1C, C_{16}); 165.83 (1C, C_{12}); 174.66 (1C, C_1). *, ** interpretations can be reversed.

2.2.3.3. *11-(Biphenyl-4-carboxamido)undecanoic acid succinimidyl ester (**IV**).* This ester was prepared in the same way as succinimidyl ester **II** (cf. § 2.2.3.1), but total elimination of *N*,*N*′-dicyclohexylurea was not possible as there is not less solubility difference between the ester and DCU. A white solid was obtained, and from the NMR spectrum one can calculate a yield of 45.0 g, 61.5% of pure ester.

FTIR: 1786, 1733, 1206, 1080 cm^{-1}. ^1H NMR (250 MHz) (DMSO d_6, 25°C): 1.27–1.7 (m, 16H, $H_{7,8,9,10,11,12,13,14}$ + DCU); 2.64 (t, 2H, H_6); 2.8 (4H, $H_{1,2}$); 3.27 (d, 2H, H_{15}); 7.49–7.9 (m, H_{arom}); 8.5 (1H, NH). ^{13}C NMR (62.8 MHz) (DMSO d_6, 25°C): 24.43 (1C, C_7); 25.57 (2C, $C_{1,2}$); 26.68 (1C, C_{13}); 28.16 (1C, C_8); 28.66 (1C, C_{12}); 28.94 (1C, C_9); 29.28 (1C, C_{10}); 30.34 (1C, C_{11}); 33.50 (1C, C_6); 34.63 (1C, C_{14}); 47.66 (DCU); 54.84 (DCU); 126.56 (2C, $C_{19,21}$); 126.96 (3C, $C_{24,26,28}$); 127.96 (2C, $C_{18,22}$); 129.14 (2C, $C_{25,27}$); 133.67 (1C, C_{17}); 139.39 (1C, C_{23}); 142.65 (1C, C_{20}); 156.8 (DCU); 165.83 (1C, C_{16}); 169.11 (1C, C_5); 170.37 (2C, $C_{3,4}$).

2.2.3.4. *11-(Biphenyl-4-carboxamido)undecanoyl-L-lysine copper complex (**V**).* In a 2 litre three-necked flask equipped with a magnetic stirrer and containing the blue solution of the lysine copper complex and 33 ml of 2M NaOH, were added, in small amounts, 44.99 g of 11-(biphenyl-4-carboxamido)undecanoic acid succinimidyl ester (0.08 mol of pure ester) suspended in 1000 ml of acetone, while the temperature was maintained at 0°C and the pH stabilized at 7–8 by addition of 2M NaOH. The system was stirred overnight, then the precipitate was filtered off, washed with water and ethanol and stored at room temperature without drying.

2.2.3.5. *11-(Biphenyl-4-carboxamido)undecanamido-L-lysine (**VI**).* The copper complex was added to a solution of 2M HCl and the system was stirred for 2 days. The suspension was filtered and the white precipitate of the lysine derivative was washed several times with water and THF.

^1H NMR (250 MHz) (DMSO d_6 + TFA d, $T = 25$°C): 1.2–1.5 (m, 20H, $H_{4,5,9,10,11,12,13,14,15,16}$); 1.85 (2H, H_3); 2.13 (t, 2H, H_8); 3.11 (t, 2H, H_{17}); 3.32 (t, 2H, H_6); 3.92 (1H, H_2); 7.5–8 (9H, H_{arom}) + DCU. ^{13}C NMR (62.8 MHz) (DMSO d_6 + TFA d, $T = 25$°C): 22.60 (1C, C_4); 26.27 (1C, C_9); 27.40 (1C, C_{15}); 29.31 (1C, C_{10}); 29.54 (1C, C_{11}); 29.85 (5C, $C_{5,12,13,14,15,16}$); 36.15 (2C, $C_{6,17}$); 52.72 (1C, C_2); 115.82 (q, $^1J_{CF} = 288.53$ Hz, TFA); 127.27* (2C, $C_{21,23}$); 127.67* (3C, $C_{26,28,30}$); 128.76 (2C, $C_{20,24}$); 129.76 (2C, $C_{27,29}$); 134.46 (1C, C_{19}); 140.31 (1C, C_{25}); 143.68 (1C, C_{22}); 159.25 (q, $^2J_{CF} = 37.91$ Hz, TFA); 166.90 (1C, C_{18}); 171.87 (1C, C_7); 174 (1C, C_1). * interpretations can be reversed.

2.3. *N-Carboxyanhydrides (NCAs)*

2.3.1. *N^{ε}-Trifluoroacetyl-L-lysine NCA*

In a 2 litre three-necked flask equipped with a magnetic stirrer, 25.82 g of N^{ε}-trifluoroacetyl-L-lysine (0.107 mol) were suspended in 1000 ml of anhydrous THF and 0.5 g of charcoal were added. Then 10 ml of diphosgene (0.083 mol, 50% excess) were added dropwise. The system was heated to 55°C, when it became clear and the temperature and stirring were maintained for 30 min. After cooling and elimination of the excess of phosgene, the NCA solution was filtered through celite, the filtrate was concentrated and the NCA was precipitated in hexane; after filtration and drying at 30°C under vacuum, 22.380 g of white NCA were obtained (yield 70.4%). The chloride content (0.92 wt %) was determined by Schales' method [4].

FTIR: characteristic anhydride vibration bands of C=O are found at 1763 and 1847 cm^{-1}. ^1H NMR (250 MHz) (DMSO d_6): 1.7–1.34 (m, 3H, $H_{4,5,6}$); 3.17 (q, 2H, H_7); 4.42 (t, 1H, H_2); 9.11* (s, 1H, H_a); 9.42* (s, 1H, H_b). * interpretations can be reversed. ^{13}C NMR (62.8 MHz) (DMSO d_6): 21.78 (1C, C_5); 27.84 (1C, C_4); 30.73 (1C, C_6); 39 (1C, C_7); 57.14 (1C, C_2); 116.16 (q, $^1J_{CF} = 288.53$ Hz, C_9); 152.17 (1C, C_3); 156.39 (q, $^2J_{CF} = 35.15$ Hz, C_8); 171.83 (1C, C_1).

2.3.2. *11-(Biphenyl-4-carboxamido)undecanamido-L-lysine NCA*

In a 2 litre three-necked flask equipped with a magnetic stirrer, 34.78 g of (biphenyl-4-carboxamido)-undecanamido-L-lysine (0.107 mol) were suspended in 1020 ml of anhydrous THF and 0.5 g of charcoal were added. Then 10 ml of diphosgene (50% excess) were added dropwise while stirring. The system was heated to 55°C. When the system became clear, the temperature and stirring were maintained for 40 min. After cooling and elimination of the excess of phosgene, the NCA solution was filtered through celite, the filtrate was concentrated, and the NCA precipitated in hexane. The NCA was dissolved in THF and precipitated in hexane

three times and finally dried in a vacuum. The required NCA derivative was obtained as a light yellow powder (28.33 g). The chloride content (1.24 wt %) was determined by Shales' method [4].

FTIR: characteristic anhydride C=O vibration bands at 1782 and 1853 cm^{-1}. ^1H NMR (250 MHz) (anhydrous DMSO d_6, $T = 25°C$): 1.1–1.7 (m, 22H, $H_{4,5,6,10,11,12,13,14,15,16,17}$); 2.02 (t, 2H, H_9); 2.99 (q, 2H, H_7); 3.25 (q, 2H, H_{18}); 4.41 (1H, H_2); 7–8 (9H, H_{arom}). ^{13}C NMR (62.8 MHz) (anhydrous DMSO d_6, $T = 25°C$): 21.87 (1C, C_5); 25.47 (1C, C_{10}); 26.66 (1C, C_{16}); 28.69–29.28 (7C, $C_{4,6,11,12,13,14,15}$); 30.78 (1C, C_{17}); 35.57 (1C, C_9); 38.15 (1C, C_7); 39.35 (1C, C_{18}); 57.14 (1C, C_2); 126.57* (2C, $C_{22,24}$); 126.98* (3C, $C_{27,29,31}$); 133.65 (1C, C_{20}); 139.37 (1C, C_{26}); 142.64 (1C, C_{23}); 152.08 (1C, C_3); 165.81 (1C, C_1); 171.83 (1C, C_{19}); 172.14 (1C, C_8) + DCU peaks. * interpretations can be reversed.

2.4. *Polymerizations*

2.4.1. *Homopolymerization*

The dry NCA was dissolved in freshly distilled DMF and then distilled hexylamine was added. A concentration of 3 wt % of NCA was used and the amount of hexylamine was determined by the degree of polymerization wanted: $\overline{DP}_n = [NCA]/[C_6NH_2]$. The polymerization was carried out at room temperature, under argon and with stirring, and was followed by SEC (GPC-disappearance of the peak for NCA) and by IR (disappearance of the characteristic bands of the anhydride at 1850 and 1780 cm^{-1}). Polymers were precipitated in water or methanol depending upon their degree of polymerization and purified by Soxhlet extraction with THF.

2.4.2. *Block copolymerization*

The first block of poly(N^{ε}-trifluoroacetyl-L-lysine) (pKt) was prepared and purified as described above. Its average number degree of polymerization was determined by titration of the terminal primary amino functions. It was then dissolved in dry DMF at a concentration of 3 wt % and the NCA of the second block was added. The polymerization of the second block was carried out at room temperature, under argon and with stirring. The block copolymers were precipitated in methanol or water and purified by Soxhlet extraction with acetone.

2.5. *Characterization techniques*

The NMR spectra were obtained using a Brucker AC 250 spectrometer operating at 250 MHz for the proton and at 62.9 MHz for the carbon 13. TMS was used as internal standard. The FTIR spectra were recorded with a Nicolet Nexus spectrometer using the KBr method.

SEC analysis (GPC) was carried out with a laboratory-made apparatus (PPS gel mixed columns, Waters 510 pump, Waters R410 refractometer, software GPChromLMOPS) using polystyrene calibration and DMF doped with LiBr at 0.1% and operating at 50°C with a flow rate of 1 ml min^{-1}.

Thermal stabilities were tested by a Du Pont TGA 2950 analyser; heating rate 10°C min^{-1} under argon. A computer interfaced Du Pont DSC 10 was used for the calorimetric analysis; heating rate 10°C min^{-1} under argon.

X-ray diffraction experiments were performed on powder samples with a laboratory-designed pinhole camera, operating under vacuum, with a Ni filtered Cu beam ($\lambda = 1.54$ Å) and equipped with a heating device for recording the diffraction patterns at various temperatures between room temperature and 300°C with an accuracy of 1°C. Several exposures were made in order to measure the strongest and the weakest reflections. Intensities of the reflections were measured with a laboratory-built microdensitometer. Experimental amplitudes of diffraction of the different orders of reflections from the smectic layers were corrected for the Lorentz polarization factor [5] and normalized so that the strongest has an amplitude of one.

3. Results

3.1. *Synthesis of L-lysine derivatives*

We have synthesized two types of L-lysine derivative: N^{ε}-trifluoroacetyl-L-lysine (Kt) and 11-(biphenyl-4-carboxamido)undecanamido-L-lysine (KC10$\phi\phi$): N^{ε}-trifluoroacetyl-L-lysine (Kt) was prepared by direct reaction of *S*-ethyl trifluorothioacetate on L-lysine monohydrochloride, as it is known that the trifluoroacetyl group becomes attached only on the ε-amino function of the lysine and not on the α-amino function [6]. Proton NMR and Carbon 13 NMR showed the purity of the Kt obtained.

In contrast, the synthesis of 11-(biphenyl-4-carboxamido)undecanamido-L-lysine (KC10$\phi\phi$) needs a more sophisticated procedure, as we showed recently that reactions on L-lysine using biphenyl derivatives such as biphenyl-4-carbonyl chloride and biphenylcarboxylic acid succinimidyl ester lead to fixation of the biphenyl both on the α- and the ε-amino functions of lysine [7]. Therefore we replaced L-lysine by its copper complex in which the α-amino function of L-lysine is protected. Therefore KC10$\phi\phi$ was prepared in five steps (figure 1): activation of the biphenylcarboxylic acid **I** in the form of its active ester **II**; aminolysis of the active ester **II** by the amine function of the 11-aminoundecanoic acid giving the acid **III**; activation of the acid **III** in the form

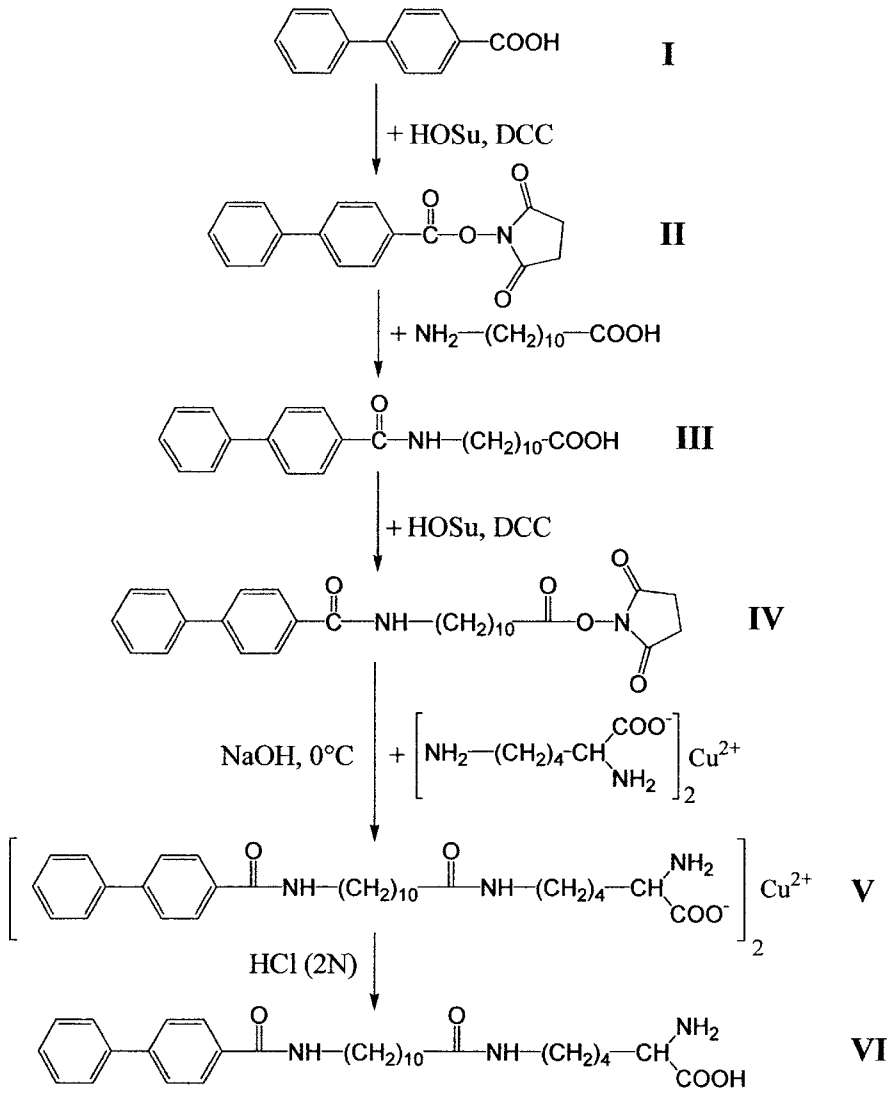

Figure 1. Scheme of synthesis for KC10ϕϕ.

of its succinimidyl ester **IV**; reaction of the active ester **IV** with the L-lysine copper complex giving the lysine derivative copper complex **V**; destruction of the copper complex **V** to obtain the L-lysine derivative **VI**.

In the first step, the biphenyl-4-carboxylic acid **I** was transformed into its succinimide ester **II** using *N*-hydroxysuccinimide (HOSu) in the presence of *N*,*N*′-dicyclohexylcarbodiimide (DCC); the precipitate of dicyclohexyl urea (DCU) formed was easily eliminated. In the second step, the ester **II** was aminolysed by the amine function of 11-aminoundecanoic acid: the reaction was performed in acetone solution in the presence of triethylamine and the biphenylcarboxamidoundecanoic acid **III** recovered by precipitation in an acidic aqueous medium. In the third step, the acid **III** was activated in the form of its succinimidyl ester **IV** using HOSu and DCC; the precipitate of DCU formed could not be eliminated totally, but its amount was determined by NMR. In the fourth step, a nucleophilic attack on the ester **IV** by the ε-amino function of the L-lysine copper complex took place; during this reaction the pH was maintained at 8 and the temperature at 0°C to obtain a good yield and avoid side reactions. The copper complex **V** was recovered as a blue precipitate. In the fifth step, the blue copper complex **V** was destroyed by pouring it into aqueous HCl and the liberated lysine derivative **VI** recovered as a white precipitate which after washing with water and THF, was analysed by IR and NMR. The yield over the five step synthesis was 36.4% of **VI**.

3.2. *Synthesis of N-carboxyanhydrides*

The N^{ε}-carboxyanhydrides (NCAs) of the two L-lysine derivatives Kt and KC10ϕϕ were synthesized by the same method. Instead of the phosgene stock solution method [8], we used, for safety reasons, liquid diphosgene

(trichloromethyl chloroformate, TCF). In the presence of activated charcoal, TCF generates phosgene on heating and an excess of 50 wt% of TCF affords a total conversion of the amino acid to its NCA [9]. Using the following conditions—solvent THF, 50 wt% excess of TCF, heating at 60°C for 40 min, crystallization from hexane (three times), characterization by IR and NMR (figure 2)—we obtained the following yields for the pure NCAs: 78.3% for Kt NCA and 50.3% for KC10ϕϕ NCA.

3.3. *Synthesis of homopolymers and copolymers*

NCAs can be polymerized by two types of initiators: primary amines and tertiary amines. Initiation by tertiary amines and strong bases leads to polymers of high molecular mass and high polydispersity [10]. Initiation by a primary amine results from nucleophilic attack by the amine on carbon C5 of the NCA and opens the anhydride ring; after rearrangement and decarboxylation this gives an amide bearing a primary amine function on the α-carbon. This amine function reacts on another molecule of NCA and produces a dimer possessing a terminal NH_2. Repetition of these reactions leads to a polymer terminated by a primary amine function and exhibiting a low polydispersity [10]. With this polymerization mechanism, the average degree of polymerization $\overline{DP}_n$ is determined by the ratio of the molar concentrations of the NCA and the primary amine:

$$\overline{DP}_n = [\text{NCA}]/[R\text{–NH}_2]$$

A further advantage of this polymerization method is the possibility of preparing block copolymers. The terminal primary amine function of the first polypeptide block is able to initiate polymerization of the NCA of the second amino acid. Therefore we have used hexylamine as initiator to prepare our homopolymers and block copolymers.

Homopolymerizations and copolymerizations were carried out at room temperature with stirring in DMF

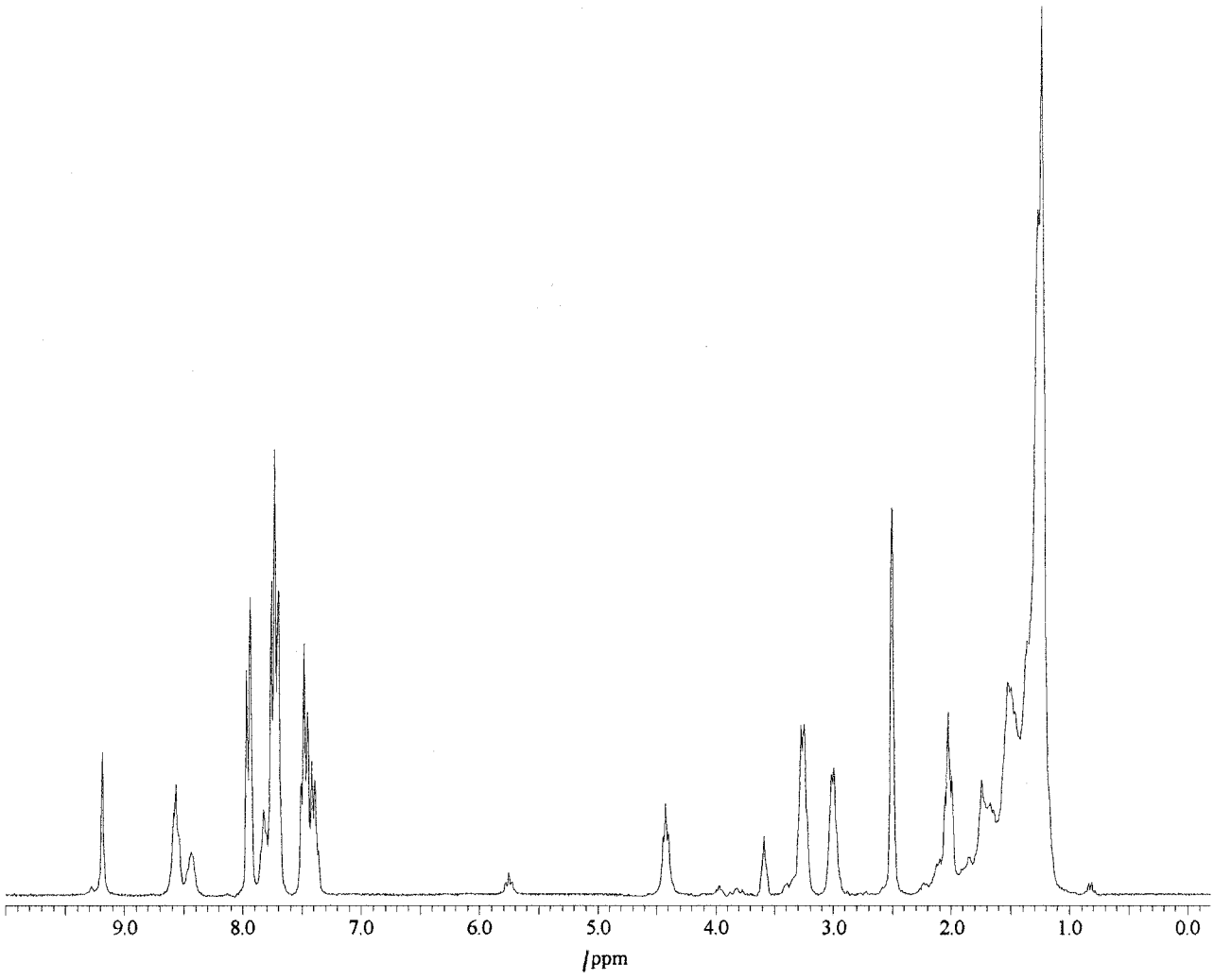

Figure 2. NMR spectra of KC10NCA at room temperature in DMSO: (*a*) proton, (*b*) carbon 13.

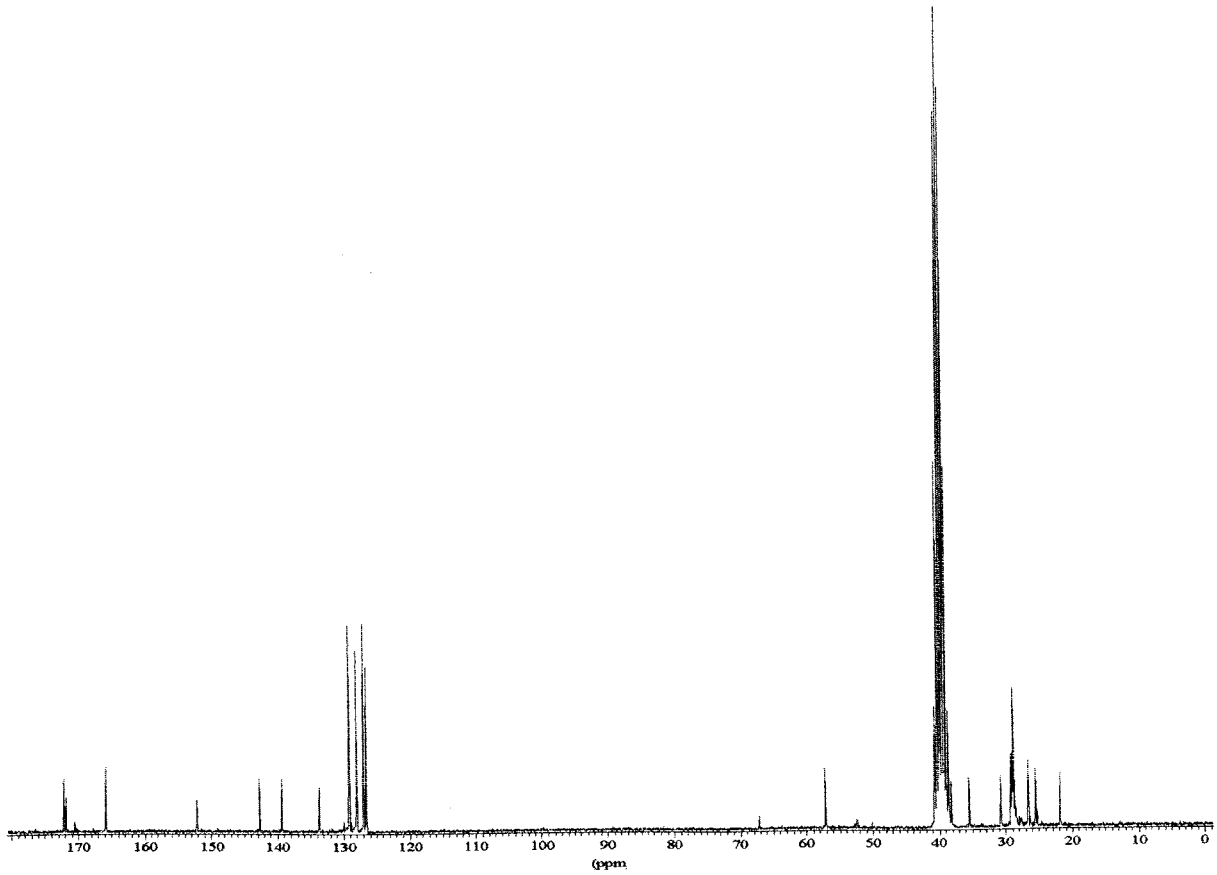

Figure 2. (*continued*).

solution. DMF is the best solvent for polypeptide synthesis, given the absence of moisture to avoid autopolymerization of the NCA [11] and an argon atmosphere to sweep out the carbon dioxide resulting from the polymerization. Polymerizations were followed by SEC (GPC) showing the disappearance of the NCA peak and by FTIR showing the disappearance of the characteristic bands of the NCA at 1850 and 1780 cm^{-1}.

At the end of a polymerization, the homopolymers were recovered by precipitation in water or methanol and purified by Soxhlet extraction with acetone for pKt and THF for pKC10ϕϕ. Yields of pure homopolymers were 74.8% for pKt and varied between 75 and 84% for pKC10ϕϕ.

Block copolymers were obtained by successive polymerization of the NCAs of the two blocks in DMF solution. The NCA of the Kt was polymerized first using hexylamine as initiator, and the pKt was precipitated, purified by Soxhlet extraction with acetone and characterized. Then the terminal amine function of the pKt was used as a macromolecular initiator for the polymerization of KC10ϕϕ NCA. The block copolymers pKt–pKC10ϕϕ were recovered by water precipitation and purified by Soxhlet extraction with acetone. The copolymer yield was only 30% because the polymer precipitation in water was not quantitative and if a lot of polymer was lost, impurities were thoroughly eliminated.

The average number molecular mass of the pKt was determined by titration of its primary amine end functions. The compositions of the block copolymers were obtained as follows. The fluorine content of the Kt block was determined and the average number molecular mass of the pKC10ϕϕ block was deduced from the molecular mass of the Kt block and the composition of the copolymer. The results are given in table 1.

Table 1. Macromolecular characteristics of the polymers.

Polymer	$\overline{DP_n}$ (pKt)[a]	%pKt in mole	$\overline{DP_n}$ (pKC10ϕϕ)[b]
pKt	77	100	0
Cop 1	77	13	515
Cop 2	77	86	13
Cop 3	77	72	30
Cop 4	77	90	7

[a] Determined by titration of NH_2 end groups.
[b] Determined from the fluorine content of the polymer.

3.4. *Liquid crystalline behaviour*

Analysis of the polymers by TGA showed that up to 300°C no weight loss occurs, so polymer structure was studied by X-ray diffraction between room temperature and 250°C to be sure that no degradation took place during the study.

3.4.1. *Determination of the liquid crystalline structures*

For all homopolymers and block copolymers, X-ray patterns recorded at temperatures between room and 250°C exhibited in the low angle region a set of sharp reflections, and in the wide angle region a diffuse band, a sharp reflection or two reflections, depending upon the polymer and the temperature. From the ratio of the Bragg spacings at low angles, X-ray diagrams can be classified into two families corresponding to structures exhibiting bidimensional hexagonal or lamellar symmetries.

3.4.1.1. *Hexagonal structure*. The first family of X-ray diagrams is characterized by the presence in the low angle domain of three sharp reflections with Bragg spacings in the ratio 1: $\sqrt{3}$: $\sqrt{4}$ (figure 3) characteristic of a bidimensional array of long rods [12]. The rods contain the peptidic chains in an α-helix conformation [13] as confirmed by FTIR spectroscopy (bands amide I at 1653 cm^{-1} and amide II at 1547 cm^{-1}), while the side chains fill the space between the helices. Such a structure is observed for the pKt homopolymers and the pKt-pKC10ϕϕ block copolymers rich in pKt (table 2).

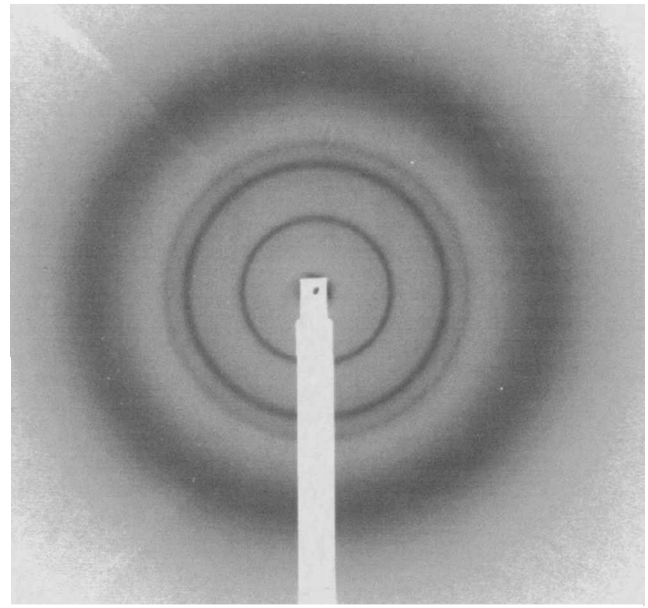

Figure 3. Example of a pin-hole camera powder X-ray diagram of the hexagonal structure for copolymer 3.

3.4.1.2. *Lamellar structure*. All X-ray diagrams typical of the lamellar structures are characterized by the presence in the low angle domain of three to five sharp reflections, but they differ in the wide angle region (see figures 4–6). The two to four reflections observed at the lowest angles can be indexed as the 0 0 l reflections of a lamellar structure of thickness *d*. The sharp reflection observed

Table 2. Structures and structural parameters of the mesophases of the homopolymers and copolymers studied between room temperature and 250°C. D_H is the parameter of the hexagonal lattice; T_1 and T_2 are transition temperatures between mesophases.

	Polymer					
Parameter	pKC10ϕϕ	Cop 1	Cop 3	Cop 2	Cop 4	pKt 8
%pKt	0	13	72	86	90	100
d or D_H/Å	57.5	60.9	62.0	14.8	14.8	14.6
a/Å	4.49	4.5	4.7			
b/Å	4.05					
θ/°	0	0	0			
Structure	CrE_d	SmA_d	SmA_d	Hexagonal	Hexagonal	Hexagonal
T_1/°C	~110	>250	~200	>250	>250	>250
d or D_H/Å	59.6		15.1			
a/Å	5.18					
θ/°	0					
Structure	SmB_d		Hexagonal			
T_2/°C	~180					
d or D_H/Å	61.8					
a/Å	4.5					
θ/°	0					
Structure	SmA_d					

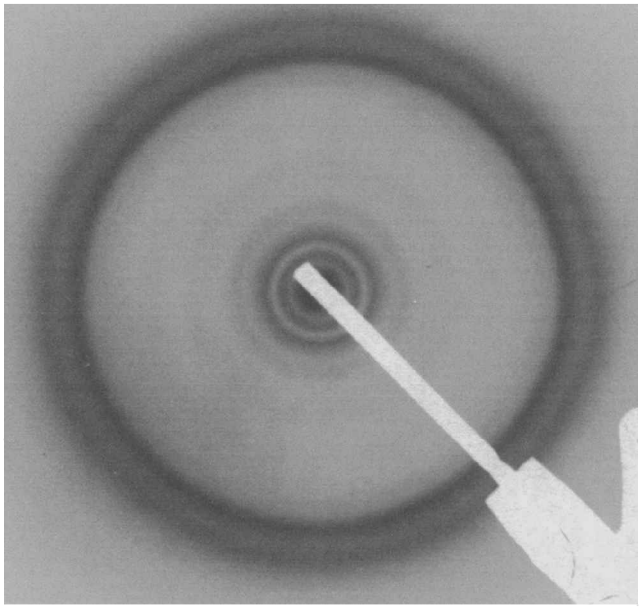

Figure 4. Example of a pin-hole camera powder X-ray diagram of the crystal smectic E structure of the first mesophase of homopolymer pKC10ϕϕ.

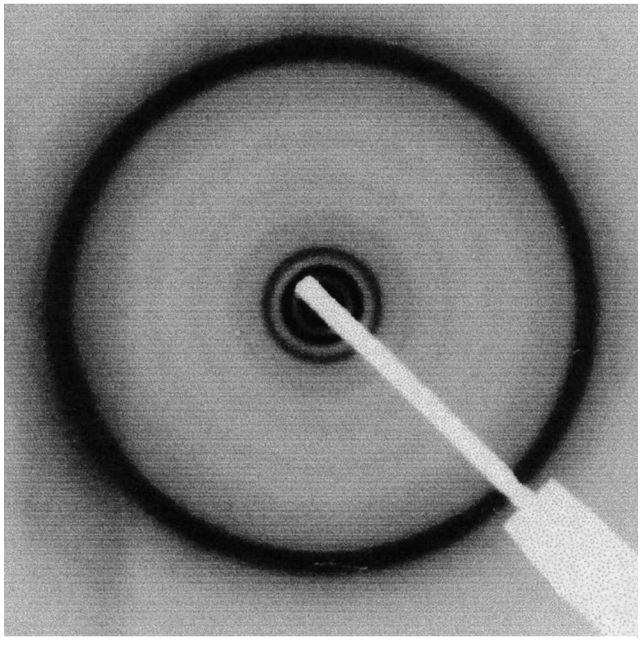

Figure 5. Example of a pin-hole camera powder X-ray diagram of the smectic B_d structure of the second mesophase of homopolymer pKC10ϕϕ.

at higher angles (repeat distance of 6.7 Å) corresponds to the β-pleated sheet periodicity of 7.0 Å (figure 7), classical for polypeptides [14] but slightly deformed by the presence of the bulky side chain. Furthermore the β-conformation is confirmed by FTIR spectroscopy (bands amide I at 1629 cm^{-1} and amide II at 1540 cm^{-1}).

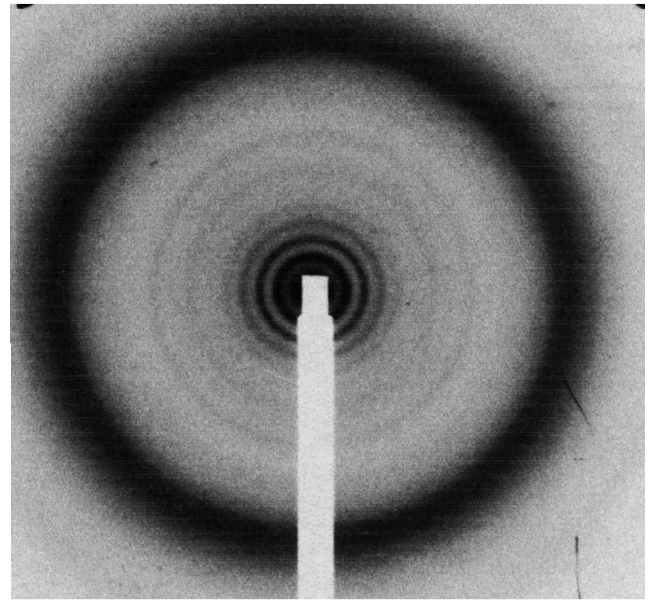

Figure 6. Example of a pin-hole camera powder X-ray diagram of the smectic A_d structure of copolymer 1.

Taking into account the signals present in the wide angle domain, the lamellar structure can be divided into three families corresponding to three different types of organization of the side chains.

(1) *Lamellar structure with rectangular organization*. This structure is characterized by the presence at wide angles of two or three reflections that can be indexed on a rectangular array of parameters $a = 4.49$ Å and $b = 4.05$ Å (see figure 4). Therefore the structure is of the ordered crystal smectic type E, H or K.

(2) *Lamellar structure with hexagonal organization*. This structure is characterized by the presence at wide angles of one sharp reflection corresponding to a hexagonal array [15] of parameter $a_H = 5.18$ Å (see figure 5). Therefore the structure is of the ordered smectic type SmB, SmF or SmI.

(3) *Disordered lamellar structure*. This structure is characterized by the presence at wide angles of a large band corresponding to a distance a between 4.5 and 4.7 Å depending on the polymer (see figure 6). Therefore the structure is of the disordered smectic type SmA or SmC.

To determine, for each family of lamellar structure, whether it is of the perpendicular or tilted type, we have compared the thickness d of the layers with the length L of the polymer repeating unit (corresponding to a monolayer structure) and the length $2l + p$ of two side chains and one main chain segment (corresponding to a bilayer structure) measured using CPK models. For all polymers we found d much higher than L ($L = 36.5$ Å),

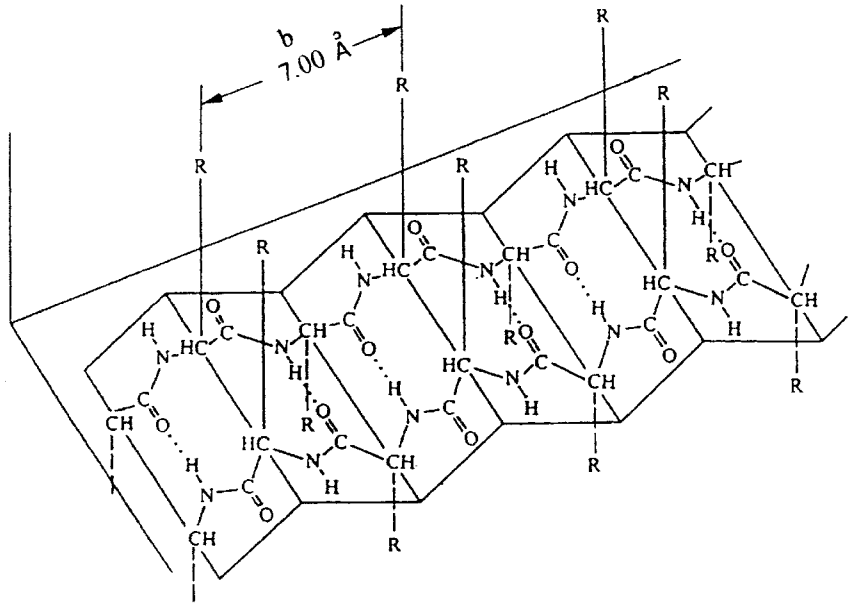

Figure 7. Schematic illustration of the antiparallel β-pleated sheet structure present in polypeptides and proteins.

but smaller than $2l + p$ ($2l + p = 69$ Å), so their structure may be of the interdigitated perpendicular smectic type or of the double layer tilted smectic type. In order to determine whether the lamellar structures are tilted smectic or perpendicular smectic, one can use the electron density profiles $\rho(z)$ along the direction z perpendicular to the smectic planes.

In order to draw electron density profiles corresponding to the perpendicular interdigitated smectics SmX_d and the tilted bilayer smectics SmX_2, we have calculated the electron densities of the different parts of the repeating unit of the polymer by dividing their numbers of electrons by their lengths measured using CPK models. We found 7.8 e-Å^{-1} for the peptidic chain, 6.4 e-Å^{-1} for the paraffinic spacer and 8.8 e-Å^{-1} for the mesogenic group. In the case of an orthogonal interdigitated structure SmX_d, the electron density profile will exhibit a central maximum corresponding to the partly interdigitated mesogenic groups, surrounded by two minima corresponding to the paraffinic spacers, and two secondary maxima corresponding to the peptidic skeleton (see figure 8). In the case of a double layer tilted smectic structure SmX_2, the electron density profile will exhibit a central minimum surrounded by two maxima corresponding to the mesogenic cores, two minima corresponding to the paraffinic spacers, and two secondary maxima corresponding to the peptidic skeleton (see figure 9).

The electron density profiles $\rho(z)$ along the direction z perpendicular to the smectic planes can be derived from the intensities of the 0 0 l low angle reflections of the X-ray patterns. Considering that equal numbers of mesogenic cores point in the $+z$ and $-z$ directions, and that we measure only the fluctuation around $\rho(0)$, the average electron density $\rho(z)$ is given by [16]:

$$\rho(z) = \sum a_n \cos(n2\pi z/d)$$

Experimentally we measure the intensity of the diffraction orders, so we lose the phase. Due to the symmetry of the electron density distribution, the phase factor and the structure factor must be 0 or π, so the a_n are real, but may be positive or negative. The phase problem then reduces to choosing the right combinations of sign for a_n ($n = 1, 2, 3 \ldots$). For instance $\rho + - + (z)$ will correspond to the combination where a_1 and a_3 are chosen positive while a_2 is chosen negative.

For the three types of smectic structures we observe three orders of diffraction with measurable intensity (corresponding to $n = 2, 3, 4$), so we obtain eight combinations of sign for a_n; that is, eight electron density profiles $\rho(z)$. As the values of a_n are very similar for the three types of smectic phase (table 3), we represent on the figures 10 (*a–h*) the eight profiles corresponding to the disordered smectic. One can compare these eight profiles with the physically acceptable ones drawn on figures 8 and 9. The four electron density profiles 10 (*e–h*) must be rejected as they exhibit maxima for the spacers and minima for the main chains, and are incompatible with

Table 3. Normalized amplitudes (a_n) of the reflections for the three smectic mesophases of homopolymers pKC10φφ.

pKC10φφ	a_1	a_2	a_3	a_4
First phase	0	1	0.45	0.10
Second phase	0	1	0.43	0.12
Third phase	0	1	0.41	0.13

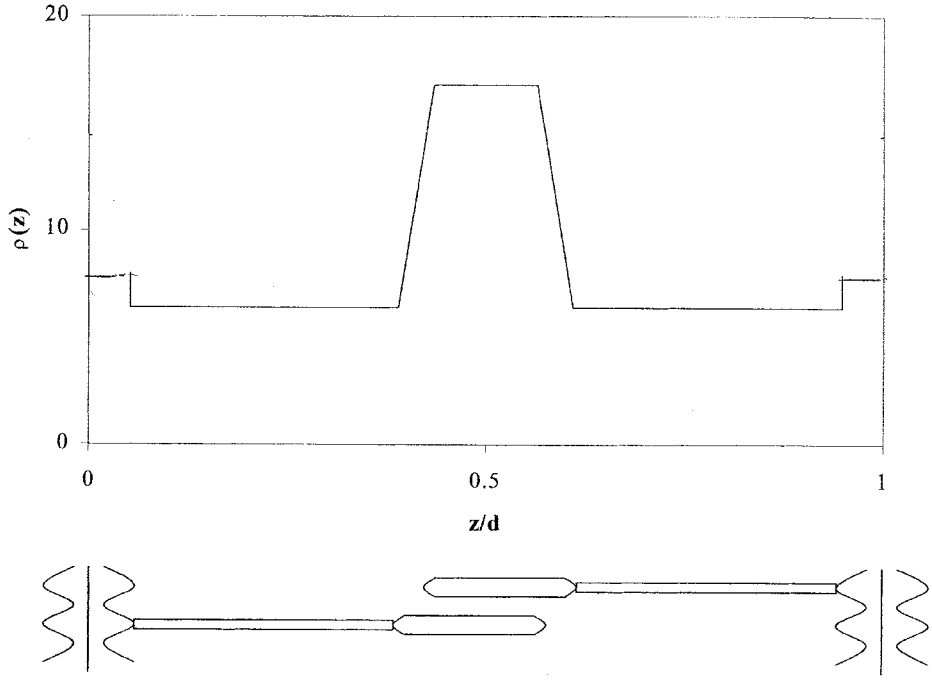

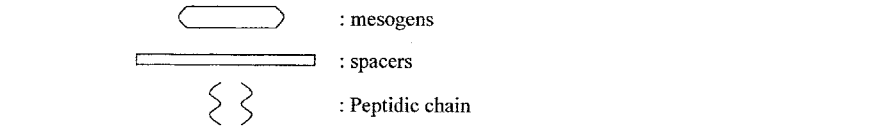

Figure 8. Schematic representation of the electron density profile of the partly interdigitated, perpendicular smectic structures SmA_d, SmB_d or E_d.

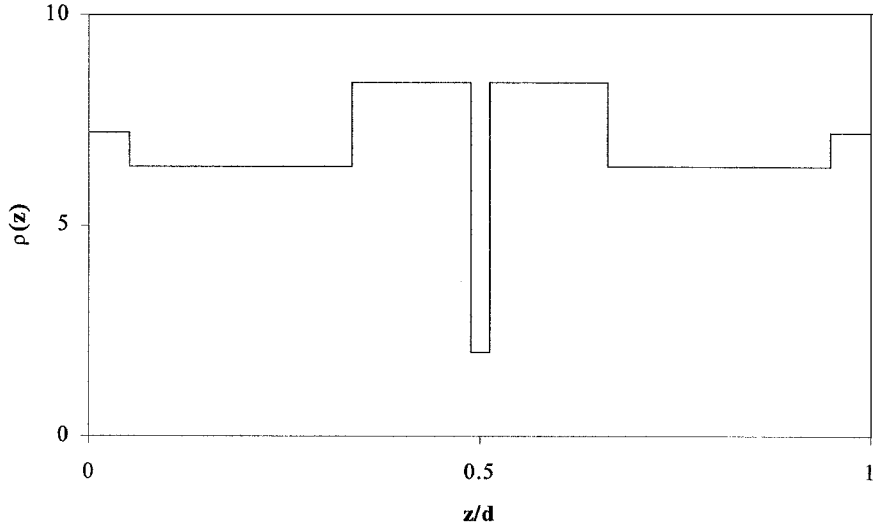

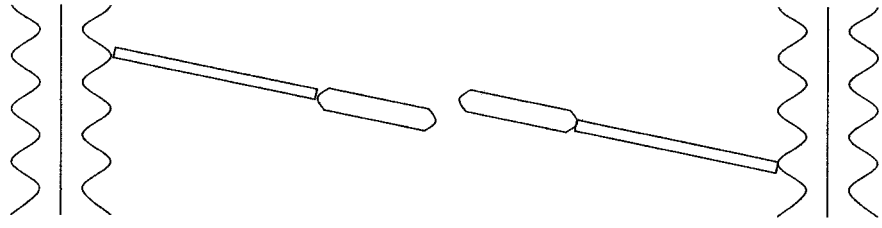

Figure 9. Schematic representation of the electron density profile of the tilted bilayer smectic structures SmC_2, SmF_2, SmI_2, H_2 or K_2.

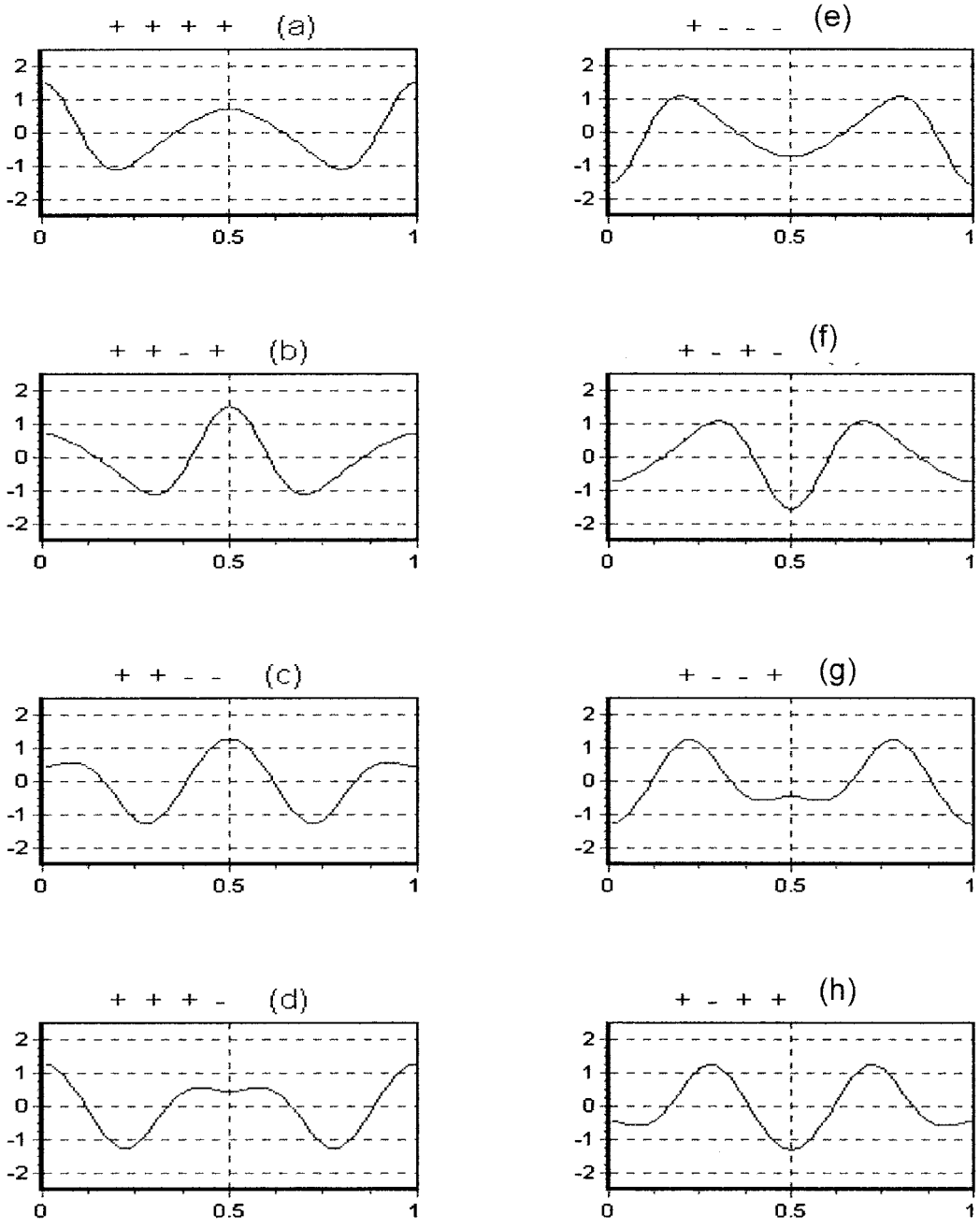

Figure 10. Projections of the electron density profiles corresponding to the eight different combinations of a_n for the third mesophase of the homopolymers pKC10$\phi\phi$.

both the double layer and the interdigitated smectic structures. The four profiles 10(*a–d*) exhibit a central maximum for the mesogenic groups, surrounded by minima for the spacers and maxima for the main chains, and are in agreement with an interdigitated perpendicular smectic SmA_d (figure 8), but are incompatible with a bilayer tilted smectic SmC_2 (figure 9). Considering that the electron density of the mesogenic groups is higher than that of the main chains, the best agreement between the experimental and the physically acceptable electron density profiles occurs for profile 10(*b*). For the smectic structures with rectangular or hexagonal organization of the side chains, the values of a_n are similar to that of the disordered smectic (table 3), so the electron density profiles are similar and the corresponding smectics are interdigitated. Therefore the three types of smectic structure are all interdigitated and are, respectively, E_d, SmB_d and SmA_d (table 2).

3.4.2. *Factors governing the liquid crystalline structures*

The main factors governing the structures of the mesophases are the polymer composition and the temperature. DSC experiments showed that among the polymers studied only the homopolymers pKC10ϕϕ and the copolymer 3 exhibit phase transitions before the start of decomposition. The homopolymers pKC10ϕϕ exhibit two transitions at 122 and 174°C and the copolymer 3 one transition at 211°C.

X-ray diffraction experiments allowed the determination of the nature of the transitions (table 2). At room temperature the homopolymers pKC10ϕϕ exhibit an interdigitated crystal smectic E_d structure. Addition of a block of pKt transforms the ordered E_d structure first into a disordered SmA_d one (Cop 1 and Cop 3) and then into a hexagonal structure when the content of pKt in the copolymer becomes high (Cop 2 and Cop 4).

When the temperature increases, the homopolymers pKC10ϕϕ exhibit an ordered rectangular crystal smectic E_d until about 110°C, then an ordered hexagonal smectic SmB_d until about 180°C and a disordered smectic SmA_d until decomposition begins at temperatures higher than 250°C. For the copolymer 1 containing 13 mol % of pKt, the disordered smectic A_d is stable until the decomposition begins. For the copolymer 3 containing 72 mol % of pKt, the disordered smectic A_d transforms at about 200°C into a hexagonal structure that remains stable until the start of decomposition. For the copolymers very rich in pKt (Cop 2 and Cop 4), the hexagonal structure remains stable until the decomposition begins, as in the case of the homopolymer pKt. Therefore the stability of the smectic structures decreases when the temperature or the content of pKt block in the polymer increases.

For any given structure the thickness *d* of the smectic layers remains unaffected by temperature, but varies abruptly at temperatures corresponding to the phase transitions on heating (*d* increases) or on cooling (*d* decreases) (see table 2).

4. Concluding remarks

In this paper we have described the synthesis and thermotropic properties of a new family of liquid crystalline polypeptides, homopolymers pKC10ϕϕ and block copolymers pKt-pKC10ϕϕ, showing that thermotropic properties can be obtained with polypeptides by introducing biphenyl groups at the end of the side chains. The polymesomorphism obtained with the biphenyl-substituted polylysines is richer than that obtained with polylysines and polyornithines bearing azobenzene mesogenic groups at the ends of their side chains. The azobenzene-modified polylysines and polyornithines exhibit only Smectic A mesophases [1–3], while biphenyl-substituted polylysines exhibit three types of mesophase (E, SmB and SmA) and even bidimensional hexagonal mesophases in the case of the block copolymers pKt-pKC10ϕϕ. It would be interesting to synthesize modified polylysines in which the azobenzene groups are linked at the end of the lysine side chains through a long spacer in order to determine the respective influences of the mesogenic unit (azobenzene or biphenyl) and the length of the spacer on the type and stability of the mesophases.

References

[1] Gallot, B., Fafiotte, M., Fissi, A., and Pieroni, O., 1996, *Makromol. Chem. rapid Commun.*, **17,** 493.
[2] Gallot, B., Fafiotte, M., Fissi, A., and Pieroni, O., 1997, *Liq. Cryst.*, **23,** 137.
[3] Gallot, B., Guillermain, C., Fissi, A., and Pieroni, O., 1999, *Mol. Cryst. liq. Cryst.*, **330,** 65.
[4] Schales, W., and Schales, A., 1965, *Ann. Chem.*, **67,** 198.
[5] *International Tables for X-ray Crystallography*, 1952 (Birmingham: Kynoch Press).
[6] Schallenberg, E., and Calvin, M., 1955, *J. Am. chem. Soc.*, **77,** 2779.
[7] Guillermain, C., and Gallot, B., *Macromol. Chem. Phys.* (submitted).
[8] Fuller, W. D., Velander, M. S., and Goodman, M., 1976, *Biopolymers*, **15,** 1869.
[9] Katakai, R., and Iisuka, Y., 1985, *J. org. Chem.*, **50,** 715.
[10] Szwarc, M., 1965, *Adv. polym. Sci.*, **4,** 1.
[11] Barlett, P., and Shalitin, Y., 1957, *J. Am. chem. Soc.*, **79,** 2153.
[12] Saludjian, P., and Luzzati, V., 1961, *J. mol. Biol.*, **15,** 981.
[13] Douy, A., and Gallot, B., 1987, *Polymer*, **28,** 147.
[14] Salemme, F. R., and Weatherford, D. W., 1981, *J. mol. Biol.*, **146,** 101, 119.
[15] De Vries, A., 1985, *Mol. Cryst. liq. Cryst.*, **131,** 125.
[16] Gudkov, V. A., 1984, *Sov. Phys. Crystallogr.*, **29,** 316.